

Enhancing Targeted Adversarial Attacks on Large Vision-Language Models through Intermediate Projector Guidance

Yiming Cao, Yanjie Li, Kaisheng Liang, Yuni Lai and Bin Xiao *Fellow, IEEE*

Abstract—Targeted adversarial attacks are essential for proactively identifying security flaws in Vision-Language Models (VLMs) before real-world deployment. However, current methods perturb images to maximize global similarity with the target text or reference image at the encoder level, collapsing rich visual semantics into a single global vector. This limits attack granularity, hindering fine-grained manipulations such as modifying a car while preserving its background. Furthermore, these methods largely overlook the projector module, a critical semantic bridge between the visual encoder and the language model in VLMs, thereby failing to disrupt the full vision-language alignment pipeline within VLMs and limiting attack effectiveness. To address these issues, we propose the Intermediate Projector Guided Attack (IPGA), the first method to attack using the intermediate stage of the projector module, specifically the widely adopted Q-Former, which transforms global image embeddings into fine-grained visual features. This enables more precise control over adversarial perturbations by operating on semantically meaningful visual tokens rather than a single global representation. Specifically, IPGA leverages the Q-Former pretrained solely on the first vision-language alignment stage, without LLM fine-tuning, which improves both attack effectiveness and transferability across diverse VLMs. Furthermore, we propose Residual Query Alignment (RQA) to preserve unrelated visual content, thereby yielding more controlled and precise adversarial manipulations. Extensive experiments show that our attack method consistently outperforms existing methods in both standard global image captioning tasks and fine-grained visual question-answering tasks in the most realistic and high-stakes black-box environment. Additionally, IPGA successfully transfers to multiple commercial VLMs, including Google Gemini and OpenAI GPT.

Index Terms—Adversarial Attack, Vision-Language Models, Projector, Q-Former.

I. INTRODUCTION

LARGE VLMs typically integrate Large Language Models (LLMs) with pretrained visual encoders via a projection module, enabling joint visual-textual reasoning [1]–[3]. They achieve strong performance on a wide range of multimodal tasks from answering general questions to task planning for AI agents and robots [4]. However, recent studies have revealed that VLMs are highly vulnerable to adversarial image attacks [5], [6], which can lead to severe consequences in downstream applications [7]. As VLMs become more accessible to the public, assessing the robustness of VLMs against such attacks is crucial prior to real-world deployment [8], [9].

While early evaluations of VLM robustness have focused on untargeted attacks [5], [6], targeted attacks pose a greater risk

by inducing specific, potentially harmful outputs [9], [10]. We investigate the more challenging setting of black-box targeted attacks against VLMs. Existing targeted image adversarial attacks on VLMs typically optimize global image embeddings to align with target text or reference image [8], [10] using pretrained encoders like CLIP [11]. These encoders are trained to maximize cosine similarity between paired global image features (e.g., the [CLS] token) and text embeddings to efficiently build a joint multimodal space. As a result, encoder-level attacks are constrained to global image content modifications, lacking the ability to manipulate specific visual features. However, in real-world applications that require fine-grained visual understanding like autonomous driving and embodied AI, coarse global perturbations are often inadequate when only specific image elements need to be altered [12]. For instance, modifying the appearance of a particular vehicle in a busy street scene without affecting surrounding content may be necessary to mislead the model’s response when identifying the target vehicle. Without such granularity, attacks lack stealth and practical effectiveness. Furthermore, encoder-level attacks overlook the projector, a critical component in VLMs that connects the visual encoder to the LLM. Trained on large-scale multimodal data, it captures alignment patterns beyond the encoder’s capacity [1]. Ignoring this stage limits the attack’s ability to disrupt the full vision-language alignment pipeline, reducing overall attack effectiveness.

To address the limitations of global, encoder-level adversarial attacks, we propose Intermediate Projector Guided Attack (IPGA), a novel targeted adversarial attack method that exploits the multimodal alignment at the projector level. We focus on the widely adopted Querying Transformer (Q-Former) projector [13]–[15], which transforms global image embeddings into fine-grained visual features via cross-attention with frozen visual encoders [1], referred to as query outputs. These query outputs capture diverse semantic aspects of the image, enabling more precise and disentangled manipulation beyond the capabilities of global feature-based methods. Specifically, we target the intermediate Q-Former projector, which has solely undergone the first pre-training stage of vision-language representation learning but has not yet been fine-tuned for LLM generation, enhancing the attack’s transferability across VLMs of various architectures. To the best of our knowledge, we are the first to demonstrate that attacking the intermediate pre-training stage of the Q-Former projector yields superior adversarial attack performance compared to focusing solely on the image and text encoders. To further preserve the unrelated content of the image, we introduce a Residual Query Alignment (RQA) module that constrains non-target query tokens to remain close to their clean counterparts, thereby enabling more

Y. Cao, Y. Li, K. Liang, Y. Lai and B. Xiao are with the Department of Computing, The Hong Kong Polytechnic University (Email: {yiming.cao, yanjie.li}@connect.polyu.hk; cskliang@comp.polyu.edu.hk; yunnie.lai@connect.polyu.hk; b.xiao@polyu.edu.hk).

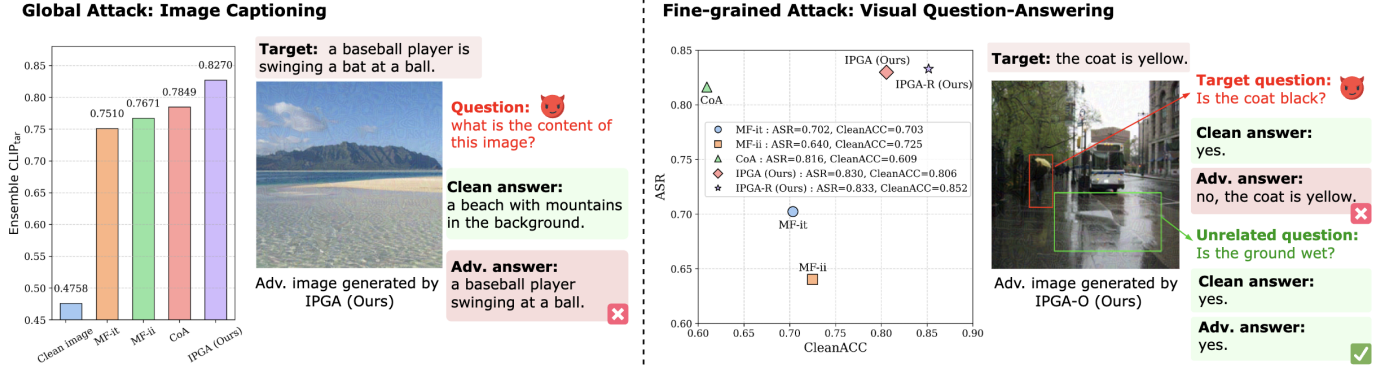


Fig. 1. Comparison of IPGA and IPGA with Residual Query Alignment (IPGA-R) against baselines on BLIP-2 [1]. Example adversarial images are included. For the global attack (left), which forces the model to recognize an adversarial image as target content, we follow prior work [8] and evaluate image captioning, reporting the ensemble CLIP similarity between the generated caption and the target text. For the fine-grained attack (right), which requires altering only the target while preserving unrelated content, we evaluate on the VQA task. Attack performance is measured by the Attack Success Rate (ASR), while preservation of unrelated content is assessed by CleanACC using unrelated questions. Results demonstrate that IPGA consistently outperforms baseline methods, and IPGA-R further improves CleanACC, enabling more precise and controlled adversarial manipulation.

controlled and precise adversarial manipulations. Following existing works [8], we evaluate global targeted adversarial attacks using ImageNet-1K [16] and MS-COCO captions [17]. We leverage the visual question-answering (VQA) task and use the GQA dataset [18] to assess the effectiveness of our approach in fine-grained attack scenarios. Our proposed IPGA consistently outperforms existing methods across both global and fine-grained attack scenarios, and incorporating RQA (IPGA-R) substantially improves the preservation of unrelated image content, enabling even more controlled and realistic adversarial manipulations in fine-grained attack scenarios, as demonstrated in Figure 1. Our attack also successfully transfers to commercial models, including Google Gemini and OpenAI GPT.

We hope the attacking strategy illustrated in this paper can encourage the future development of more trustworthy VLMs and their adversarial robustness evaluations. Our contributions are summarized as follows:

- We propose Intermediate Projector Guided Attack (IPGA), a novel targeted adversarial attack that operates at the projector level of vision-language models (VLMs). Specifically, we leverage the intermediate Q-Former projector trained solely in the first pre-training stage. This opens a new attack surface and achieves superior attack performance and transferability across VLMs.
- We leverage the Q-Former’s ability to transform global image embeddings into fine-grained visual tokens to improve attack granularity. Our method enables fine-grained adversarial manipulation that achieves the desired target output while preserving unrelated visual content.
- We introduce Residual Query Alignment (RQA), which encourages query tokens unrelated to the target to remain close to their clean counterparts, further improving preservation of unrelated content and enabling controlled adversarial manipulation.
- Extensive experiments demonstrate that IPGA surpasses existing targeted attack methods, revealing critical vulnerabilities in VLMs. We further demonstrate its transferability to commercial VLMs such as OpenAI GPT and

Google Gemini.

II. RELATED WORK

A. Vision-Language Models (VLMs) and Projectors

Large Vision-Language Models (VLMs) [1], [19] leverage large-scale pretrained models for superior performance in various multimodal tasks, including image captioning [20], [21] and visual question-answering [2], [22]. Architecturally, VLMs generally consist of three components: a pretrained visual encoder (e.g., CLIP [11] in LLaVA [2] or EVA-CLIP [23] in InstructBLIP [13]), a pretrained LLM, and a learnable projector [6], also known as a vision adapter [24], which connects the visual encoder to the LLM by mapping image embeddings into the LLM’s embedding space to produce modality-aligned visual features. There are two predominant projector architectures. Linear projectors [2], [3], [25] directly map visual features into the word embedding space. Cross-attention-based projectors, exemplified by the Q-Former [1], [13], [14], use learnable query embeddings to attend to image features via cross-attention, and with text via self-attention, yielding fine-grained visual tokens aligned with textual representations. Projectors are typically trained in two stages [1]–[3], [13], [24]: an initial vision-language pretraining stage using vast corpus of image-text pairs to align visual features with language representations, generally with the LLM frozen, followed by supervised fine-tuning with the LLM for generation and instruction-following. Q-Former follows a similar two-stage pipeline: it is first trained to extract semantically rich visual features via tasks like image-text contrastive learning and captioning, then connected to a frozen LLM during fine-tuning to enable vision-conditioned generation.

B. Adversarial Attacks on VLMs

Adversarial attacks introduce imperceptible perturbations to inputs, causing models to produce incorrect predictions [26]. They are categorized as untargeted or targeted based on the adversary’s objective, and as white-box or black-box based

on the attacker’s knowledge [26]. White-box attacks assume full access to model parameters [27], while black-box attacks rely on transfer-based [28] or query-based methods [29]. Most adversarial attacks on VLMs are untargeted, aiming to degrade general performance [5], [6], [30], [31]. In contrast, targeted attacks manipulate model outputs toward specific adversarial goals. Recently, AttackVLM [8] use pretrained encoders like CLIP [11] as surrogates, generating adversarial images by aligning global image embeddings with target image representations. Chain-of-Attack [10] leverages modality fusion between embeddings from a surrogate image encoder and text encoder, updating multimodal semantics at each step to enhance adversarial example generation. Generator-based approaches [32] optimize perturbation generators via pretraining and fine-tuning. However, all these approaches optimize global image embeddings at the encoder level. This limits attacks to coarse modifications and lacks the granularity needed to manipulate specific visual elements. Moreover, they ignore the projector module, which plays a critical role in aligning visual features with language models in VLMs, further reducing attack effectiveness. In this paper, we leverage the stage-1 pretrained Q-Former projector, which extracts fine-grained visual features via query-based cross-attention, enabling more precise and effective targeted perturbations.

III. PRELIMINARIES

A. Problem Settings

Let M represent the victim VLM, $\mathbf{x} \in \mathbb{R}^{3 \times H \times W}$ represent the input image, and \mathbf{t}_{in} the input text. Adversarial image attacks aim to modify the visual input to generate adversarial example \mathbf{x}_{adv} by a perturbation δ and induce M to output the targeted textual response \mathbf{t}_{tar} . This can be formalized as:

$$\begin{aligned} M(\mathbf{x}_{\text{adv}}, \mathbf{t}_{\text{in}}) &= \mathbf{t}_{\text{tar}}, \text{ where} \\ \mathbf{x}_{\text{adv}} &= \mathbf{x}_{\text{clean}} + \delta \text{ subject to } \|\delta\|_{\infty} \leq \epsilon, \end{aligned} \quad (1)$$

where ϵ represents the maximum allowed magnitude of perturbations under the l_{∞} -norm, ensuring imperceptibility. While most existing targeted attacks manipulate the overall semantics of the image, real-world applications such as embodied AI and autonomous driving often demand finer control over visual content. Beyond global attacks, which induce entirely unrelated outputs, we further investigate the more challenging and less explored fine-grained setting, where the goal is to modify specific objects or attributes while preserving unrelated visual context. For image captioning, the targeted response \mathbf{t}_{tar} describes the targeted global image content, whereas for VQA, the targeted response \mathbf{t}_{tar} corresponds to a specific answer to the given question. We address the most realistic and challenging threat model, where the adversary has black-box access to the victim model and has a targeted attack goal.

B. Querying Transformer (Q-Former)

Querying Transformer (Q-Former) is a widely adopted projector in VLMs that connects a frozen visual encoder to a frozen LLM [1], [13]. It consists of two transformer submodules that share the same self-attention layers: an image transformer f_{ϕ} , which applies cross-attention between image

embeddings and a set of learnable query tokens, and a text transformer f_{ψ} , which functions as a text encoder or decoder depending on the task. Given an input image \mathbf{x} , Q-Former takes the image embeddings $g_{\phi}(\mathbf{x})$ from a frozen visual encoder and a set of 32 learnable query tokens $\{\mathbf{q}_i\}_{i=1}^{32} \in \mathbb{R}^{32 \times d}$ as input. Through cross-attention, these query tokens attend to different parts of the image and extract a set of fine-grained, semantically meaningful visual representations, referred to as query outputs:

$$\{\mathbf{q}_i^{\mathbf{x}}\}_{i=1}^{32} = f_{\psi}(\{\mathbf{q}_i\}, g_{\phi}(\mathbf{x})) \in \mathbb{R}^{32 \times d} \quad (2)$$

These query outputs are then passed to the LLM along with the input text tokens. We denote the query outputs from clean and adversarial images as $\{\mathbf{q}_i^{\text{clean}}\}$ and $\{\mathbf{q}_i^{\text{adv}}\}$, respectively. Q-Former is trained in two stages: in stage 1, it is trained on image-text pairs to enable the query tokens to extract visual representations most informative for the associated text; in stage 2, it is fine-tuned with a frozen LLM for vision-conditioned generation.

IV. METHODOLOGY

The main framework of IPGA is illustrated in Figure 2. We exploit the stage-1 Q-Former query outputs, which encode fine-grained visual features for image-text contrastive learning, image-grounded text generation, and image-text matching with target text, to enhance targeted attack performance and granularity. In the following, we will first present the proposed Intermediate Projector Guided Attack (IPGA), followed by the Residual Query Alignment (RQA) module, which further improves the preservation of unrelated content in fine-grained targeted attacks.

A. Intermediate Projector Guided Attack (IPGA)

Our proposed Intermediate Projector Guided Attack (IPGA) leverages the stage-1 pretrained Q-Former and its corresponding encoder as a surrogate model. Stage-1 Q-Former extracts fine-grained visual features aligned with text while being independent of any specific LLM, which enhances the transferability of adversarial perturbations. IPGA is guided by three losses derived from Q-Former’s stage-1 training objectives: image-text contrastive loss (\mathcal{L}_{ITC}), image-grounded text generation loss (\mathcal{L}_{ITG}), and image-text matching loss (\mathcal{L}_{ITM}). To further boost performance on global targeted attacks, we additionally incorporate encoder-level alignment as a supplementary loss.

Image-text contrastive learning loss (\mathcal{L}_{ITC}) \mathcal{L}_{ITC} encourages the query outputs from the adversarial image $\{\mathbf{q}_i^{\text{adv}}\}$ to align with the target text embedding \mathbf{e}^{tar} , while pushing them away from the clean text embedding $\mathbf{e}^{\text{clean}}$. \mathbf{e}^{tar} and $\mathbf{e}^{\text{clean}}$ are the [CLS] token embeddings of the target and clean texts obtained from the text transformer f_{ψ} . Instead of aligning global image features with text as in prior work, we compute the similarity between each query output and the text embedding, selecting the query output with the highest similarity as the most discriminative visual feature for optimization. The loss \mathcal{L}_{ITC} is defined as:

$$\mathcal{L}_{\text{ITC}} = \gamma \cdot s_{\text{clean}} - s_{\text{tar}}, \text{ where} \quad (3)$$

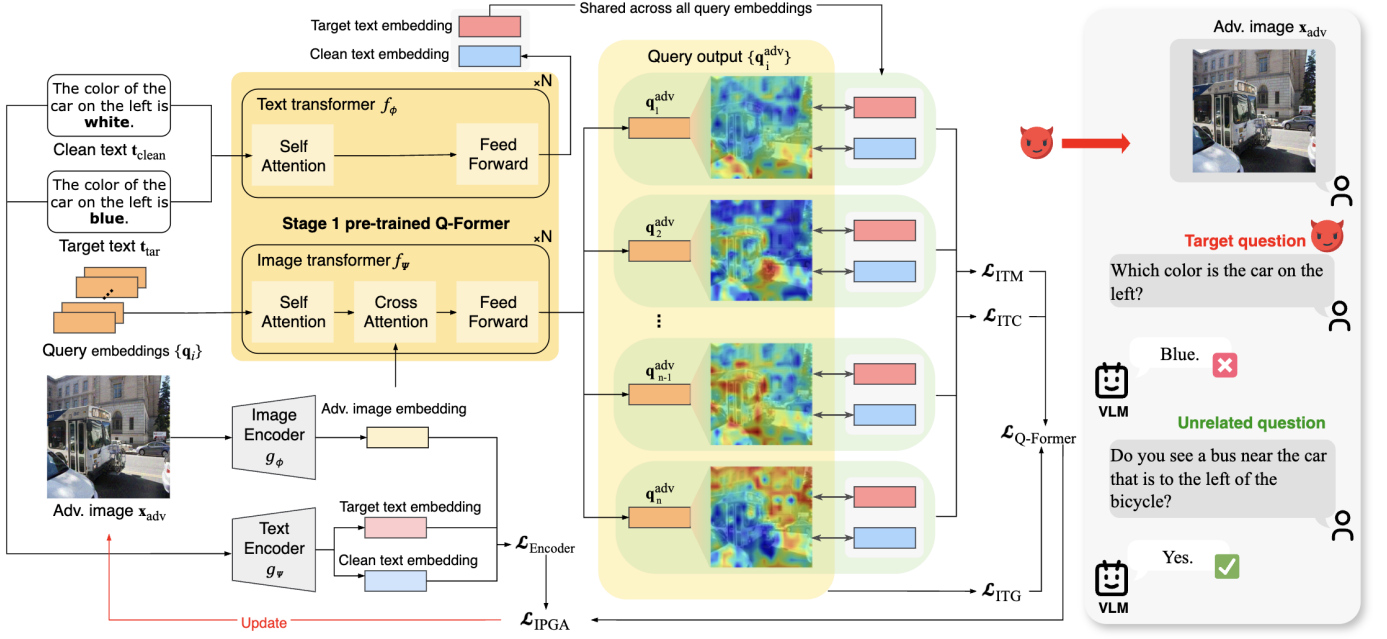


Fig. 2. The framework of our proposed Intermediate Projector Guided Attack (IPGA). IPGA leverages the stage-1 pretrained Q-Former projector and its corresponding encoder as a surrogate model. The stage-1 Q-Former is chosen for its ability to extract fine-grained visual features aligned with textual representations, independent of any specific LLM, which enhances the transferability of adversarial perturbations. The attack adapts Q-Former’s pretraining objectives, including image-text contrastive learning, image-grounded text generation and image-text matching to generate adversarial images.

$$s_{\text{tar}} = \max_i \frac{\mathbf{q}_i^{\text{adv}} \cdot \mathbf{e}^{\text{tar}}}{\|\mathbf{q}_i^{\text{adv}}\| \|\mathbf{e}^{\text{tar}}\|}, \quad (4)$$

$$s_{\text{clean}} = \max(\max_i \frac{\mathbf{q}_i^{\text{adv}} \cdot \mathbf{e}^{\text{clean}}}{\|\mathbf{q}_i^{\text{adv}}\| \|\mathbf{e}^{\text{clean}}\|} - s_{\text{tar}}, 0) \quad (5)$$

where γ is a hyperparameter to balance the influence of the clean text signal and is shared across all three losses.

Image-grounded text generation loss (\mathcal{L}_{ITG}). \mathcal{L}_{ITG} aims to generate target text conditioned on the adversarial image features extracted by all the query outputs $\{\mathbf{q}_i^{\text{adv}}\}$. We maximize the probability of generating \mathbf{t}_{tar} while minimizing the probability of generating $\mathbf{t}_{\text{clean}}$. Let l denote the cross-entropy loss for language generation. The loss \mathcal{L}_{ITG} is defined as:

$$\mathcal{L}_{\text{ITG}} = -\gamma \cdot u_{\text{clean}} + u_{\text{tar}}, \text{ where} \quad (6)$$

$$u_{\text{tar}} = l(f_{\psi}(\{\mathbf{q}_i^{\text{adv}}\}), \mathbf{t}_{\text{tar}}), \quad (7)$$

$$u_{\text{clean}} = \max(l(f_{\psi}(\{\mathbf{q}_i^{\text{adv}}\}), \mathbf{t}_{\text{clean}}) - u_{\text{tar}}, 0) \quad (8)$$

Image-text matching loss (\mathcal{L}_{ITM}). \mathcal{L}_{ITM} drives the adversarial image to match the target text while mismatching the clean text. Let $\{Q_{\text{cond}}(\mathbf{x}, \mathbf{t})_i\}$ denote the set of query outputs obtained by attending learnable queries $\{\mathbf{q}_i\}$ to frozen image features $g_{\phi}(\mathbf{x})$ via cross-attention and to text embeddings $f_{\psi}(\mathbf{t})$ via shared self-attention. Each query output $Q_{\text{cond}}(\mathbf{x}, \mathbf{t})_i$ is passed through a two-class classifier h to produce a logit; these logits are averaged across queries to produce the final matching score. Let \mathbb{E}_i denote expectation over query indices, and l_{cls} be the binary cross-entropy loss. The loss is defined as:

$$\mathcal{L}_{\text{ITM}} = \gamma \cdot l_{\text{cls}}(v(\mathbf{t}_{\text{clean}}), 0) + l_{\text{cls}}(v(\mathbf{t}_{\text{tar}}), 1), \text{ where} \quad (9)$$

$$v(\mathbf{t}) = \mathbb{E}_i [h(Q_{\text{cond}}(\mathbf{x}_{\text{adv}}, \mathbf{t})_i)] \quad (10)$$

Overall loss with Q-Former ($\mathcal{L}_{\text{Q-Former}}$). The final adversarial objective for Q-Former-based perturbation generation combines the three projector-level losses:

$$\mathcal{L}_{\text{Q-Former}} = \mathcal{L}_{\text{ITC}} + \mathcal{L}_{\text{ITG}} + \mathcal{L}_{\text{ITM}} \quad (11)$$

Intermediate projector guided attack loss ($\mathcal{L}_{\text{IPGA}}$). To further strengthen the attack, we incorporate an encoder-level alignment loss as a supplementary component for global targeted attacks where the goal is to disrupt the entire content of the image. Let g_{ϕ} and g_{ψ} denote the image and text encoders. $\mathcal{L}_{\text{Encoder}}$ encourages the adversarial image to align with the target text while diverging from the clean text:

$$\mathcal{L}_{\text{Encoder}} = \beta \cdot z(\mathbf{t}_{\text{clean}}) - z(\mathbf{t}_{\text{tar}}), \text{ where} \quad (12)$$

$$z(\mathbf{t}) = \frac{g_{\phi}(\mathbf{x}_{\text{adv}}) \cdot g_{\psi}(\mathbf{t})}{\|g_{\phi}(\mathbf{x}_{\text{adv}})\| \|g_{\psi}(\mathbf{t})\|} \quad (13)$$

The total loss $\mathcal{L}_{\text{IPGA}}$ is then expressed as:

$$\mathcal{L}_{\text{IPGA}} = \alpha \cdot \mathcal{L}_{\text{Q-Former}} + (1 - \alpha) \cdot \mathcal{L}_{\text{Encoder}} \quad (14)$$

where $\alpha \in [0, 1]$ controls the trade-off between $\mathcal{L}_{\text{Q-Former}}$ and $\mathcal{L}_{\text{Encoder}}$. In global attacks, when the target is to disrupt the entire original content of the image, we retain $\mathcal{L}_{\text{Encoder}}$. For fine-grained attacks, where the target is to modify specific objects or attributes while preserving the rest context (e.g., altering a specific pedestrian or road sign in autonomous driving), we set $\alpha = 1$, optimizing only the Q-Former loss without the encoder-level alignment loss.

B. Residual Query Alignment (RQA) for Fine-Grained Attack

Although Q-Former loss enables fine-grained adversarial optimization by disentangling visual semantics across query outputs, such optimization can inadvertently alter regions of the image unrelated to the attack target. To mitigate this and improve content preservation, we introduce Residual Query Alignment (RQA), which constrains query outputs that are semantically irrelevant to the target text.

We first compute the cosine similarity between each adversarial query output $\mathbf{q}_i^{\text{adv}}$ and the target text embedding \mathbf{e}^{tar} . The indices of the top- k most semantically relevant queries are then selected as:

$$\mathcal{I}_{\text{sem}} = \text{TopK_indices}_i\left(\frac{\mathbf{q}_i^{\text{adv}} \cdot \mathbf{e}^{\text{tar}}}{\|\mathbf{q}_i^{\text{adv}}\| \|\mathbf{e}^{\text{tar}}\|}\right) \quad (15)$$

where $\text{TopK_indices}_i(\cdot)$ denotes that we select the query output indices corresponding to the top- k similarity scores. The remaining queries that are semantically unrelated to the target are defined as residual queries:

$$\mathcal{I}_{\text{res}} = \{0, \dots, 31\} \setminus \mathcal{I}_{\text{sem}} \quad (16)$$

To reduce the effect of adversarial perturbations on unrelated regions, we regularize the residual queries to remain close to their clean counterparts:

$$\mathcal{L}_{\text{res}} = \sum_{i \in \mathcal{I}_{\text{res}}} \|\mathbf{q}_i^{\text{adv}} - \mathbf{q}_i^{\text{clean}}\|_2^2 \quad (17)$$

The final objective combines the IPGA loss with Residual Query Alignment (IPGA-R) is formulated as:

$$\mathcal{L}_{\text{IPGA-R}} = \mathcal{L}_{\text{IPGA}} + \lambda \cdot \mathcal{L}_{\text{res}} \quad (18)$$

where λ controls the strength of regularization. This module explicitly constrains the residual queries that are semantically unrelated to the target to remain close to their clean counterparts, thereby further enhancing the preservation of unrelated image content.

V. EXPERIMENTS

A. Experimental Setup

Datasets. For the evaluation of global targeted attack on image captioning task, following previous works [8], we use the validation images from ImageNet-1K [16] as clean images, and randomly select a text description from MS-COCO captions [17] as the targeted text for each clean image. For the fine-grained targeted attack evaluation on the VQA task, we utilize question-answer pairs from the balanced validation set of GQA [18]. For each image, we select one question as the targeted VQA question and use GPT-4o [19] to generate a false answer as the target text. To assess whether unrelated image content is preserved, we pair each targeted question with an unrelated clean question from GQA, use its corresponding ground-truth answer.

Victim VLMs. We evaluate SOTA open-source VLMs of varying sizes and architectures, including BLIP-2 [1], InstructBLIP [13], MiniGPT-4 [14], LLaVA [2], and LLaVA-NeXT [25], with parameter sizes ranging from 7B (BLIP-2) to 72B (LLaVA-NeXT). While BLIP-2, InstructBLIP, and MiniGPT-4 employ the Q-Former projector, they are fine-tuned on distinct tasks and LLMs. In contrast, LLaVA and LLaVA-NeXT adopt a linear projector without the Q-Former architecture.

Baselines. We compare IPGA with existing transfer-based targeted attack baselines: including MF-it [8], which optimizes cross-modal similarity by aligning image-text features, MF-ii [8], which optimizes image-image similarity by generating reference images via a text-to-image model, Chain-of-Attack (CoA) [10], which updates the multi-modal semantics and generate the adversarial examples based on their previous semantics.

Evaluation metrics. For global attacks, we follow previous works [8] and measure the similarity between the generated response and the predefined target text using various CLIP text encoders. For fine-grained attacks, we evaluate the Attack Success Rate (ASR). To assess whether unrelated image content is preserved, we measure the accuracy of unrelated clean questions as CleanACC.

Implementation details. Following prior work [8], we set $\epsilon = 8$ under the l_∞ norm to ensure adversarial perturbations remain visually imperceptible, with pixel values in the range [0, 255]. We employ NI-FGSM [33] for optimization, using 200 steps for our method and other gradient-based baselines, with an attack step size of $1/255$, as this configuration consistently yields optimal performance across all methods. For baseline methods MF-it, MF-ii, and CoA, we use the same vision encoder as the open-source victim VLM as surrogate model. We pair the same vision encoder with the stage-1 pretrained Q-Former as surrogate model for our IPGA. Hyperparameters are set as follows unless otherwise specified: For global attacks on image captioning, we use $\alpha = 0.25$, $\beta = 0.5$, and $\gamma = 1$, leveraging both Q-Former and encoder-level losses for effective global attack. For fine-grained attacks on visual question answering, we set $\alpha = 0$ and $\gamma = 1$, focusing solely on the Q-Former loss to target specific visual elements while preserving unrelated image content. For residual query alignment in fine-grained attacks, we set the regularization strength $\lambda = 1 \times 10^{-4}$ and select the top- $k = 3$ semantically relevant query outputs. All experiments are conducted using PyTorch on eight NVIDIA GeForce RTX 3090 Ti GPUs.

B. Main Experiments

Quantitative results of global attack performance. In Table I, we evaluate the effectiveness of IPGA in generating black-box adversarial images against VLMs for the image captioning task. In this setting, the adversarial attack aims to completely alter the image’s semantic interpretation, causing the model to generate a randomly predefined target caption.

To conduct this evaluation, we sample 1,000 clean images from the ImageNet-1K validation set and assign each image a randomly selected target text from MS-COCO captions.

TABLE I

BLACK-BOX ATTACKS AGAINST VICTIM MODELS IN IMAGE CAPTIONING. WE SAMPLE CLEAN IMAGES FROM THE IMAGENET-1K VALIDATION SET AND RANDOMLY SELECT A TARGET TEXT FROM MS-COCO CAPTIONS FOR EACH CLEAN IMAGE. WE REPORT THE CLIP SCORE (\uparrow) BETWEEN THE GENERATED RESPONSES OF INPUT IMAGES AND PREDEFINED TARGETED TEXTS, AS COMPUTED BY VARIOUS CLIP TEXT ENCODERS AND THEIR ENSEMBLE (AVERAGE). FOR REFERENCE, WE ALSO REPORT THE NUMBER OF PARAMETERS OF VICTIM MODELS. THE BOLD NUMBERS INDICATE THE BEST RESULTS, WHILE THE GRAY SHADING INDICATES OUR PROPOSED METHOD.

VLM model	Attack method	Text encoder (pretrained) for evaluation						# Param.
		RN50 \uparrow	RN101 \uparrow	ViT-B/32 \uparrow	ViT-B/16 \uparrow	ViT-L/14 \uparrow	Ensemble \uparrow	
BLIP2	Clean image	0.4945	0.4714	0.5279	0.5071	0.3781	0.4758	7B
	MF-it	0.7614	0.7455	0.7819	0.7705	0.6960	0.7511	
	MF-ii	0.7762	0.7618	0.7973	0.7873	0.7126	0.7670	
	CoA	0.7942	0.7822	0.8138	0.8022	0.7323	0.7849	
	IPGA	0.8347	0.8237	0.8505	0.8414	0.7846	0.8269	
InstructBLIP	Clean image	0.5105	0.4792	0.5463	0.5244	0.3925	0.4906	13B
	MF-it	0.7452	0.7274	0.7665	0.7537	0.6712	0.7328	
	MF-ii	0.7564	0.7381	0.7799	0.7663	0.6841	0.7449	
	CoA	0.7599	0.7399	0.7838	0.7700	0.6889	0.7485	
	IPGA	0.8158	0.7997	0.8327	0.8232	0.7560	0.8055	
MiniGPT-4	Clean image	0.4075	0.4351	0.4657	0.4187	0.2983	0.4051	14B
	MF-it	0.6648	0.7045	0.7200	0.6884	0.6156	0.6787	
	MF-ii	0.6776	0.7186	0.7332	0.7018	0.6324	0.6927	
	CoA	0.6926	0.7316	0.7478	0.7168	0.6485	0.7075	
	IPGA	0.7387	0.7713	0.7849	0.7603	0.6970	0.7505	
LLaVA	Clean image	0.4678	0.4581	0.4881	0.4770	0.3419	0.4466	13B
	MF-it	0.6751	0.6699	0.6977	0.6913	0.6025	0.6673	
	MF-ii	0.6968	0.6939	0.7208	0.7102	0.6239	0.6891	
	CoA	0.6998	0.6952	0.7235	0.7128	0.6211	0.6905	
	IPGA	0.7175	0.7126	0.7394	0.7296	0.6411	0.7080	
LLaVA-NeXT	Clean image	0.4500	0.4406	0.4755	0.4537	0.3276	0.4295	72B
	MF-it	0.6194	0.6177	0.6472	0.6305	0.5372	0.6104	
	MF-ii	0.6308	0.6243	0.6524	0.6399	0.5446	0.6184	
	CoA	0.6087	0.6058	0.6391	0.6206	0.5190	0.5986	
	IPGA	0.6384	0.6365	0.6663	0.6510	0.5591	0.6305	

Target: A blue passenger train on a track next to a large bush.

Target: Two men and a women are in the water at the beach while playing Frisbee.

Target: A group of tie racks with men's ties on them .



(Clean) A small white and brown dog sitting in a field surrounded by green plants and flowers.

(Adv.) A blue train traveling on a track next to a large tree with purple flowers.

(a) MiniGPT-4

(Clean) A black rocking chair with a fur blanket on it.

(Adv.) A group of people playing frisbee in the water.

(b) LLaVA

(Clean) A young girl riding a brown horse in a field.

(Adv.) A man standing next to a group of wooden tie racks.

(c) LLaVA-NeXT

Fig. 3. Visualization of the attack results of our IPGA on various open-source VLMs. We show the adversarial target text above the image, and display the image caption results of original image and adversarial example below the image.

Following previous works [8], we report the CLIP score, which measures the similarity between the generated responses and the predefined target texts. The scores are computed using various CLIP text encoders, as well as their ensemble average. The default input prompt is fixed to be “what is the content of this image?”. The original text for each image is generated using the default input prompt and the original clean image on BLIP2. Our experiments reveal that IPGA consistently outperforms all baseline methods, achieving a higher CLIP score across all evaluated models. Despite LLaVA and LLaVA-NeXT not utilizing a Q-Former projector, IPGA still achieve the highest CLIP scores among all baselines.

This indicates that adversarial attacks generated using the intermediate Q-Former exhibit strong transferability to VLMs with different architectures. Finally, we observe a general trend where larger VLMs exhibit greater robustness against targeted adversarial attacks, indicating that model scale may play a role in adversarial resistance.

Qualitative results of global attack performance. As shown in Figure 3, we present visualizations of our method’s attacks on open-source VLMs, including MiniGPT-4, LLaVA, and LLaVA-NeXT, which encompass diverse architectures; notably, LLaVA and LLaVA-NeXT do not incorporate a Q-Former module. Using a small perturbation budget of $\epsilon =$

TABLE II

BLACK-BOX ATTACKS AGAINST VICTIM MODELS IN VISUAL QUESTION ANSWERING. WE SAMPLE CLEAN IMAGES FROM THE GQA VALIDATION SET AND USE GPT-4o TO GENERATE A FALSE, UNRELATED ANSWER AS THE TARGETED ANSWER. WE REPORT THE ATTACK SUCCESS RATE (ASR)(\uparrow) FOR THE TARGETED QUESTIONS AND THE ACCURACY ON CLEAN SAMPLES (CleanACC)(\uparrow). THE BOLD NUMBERS INDICATE BETTER RESULTS, WHILE THE GRAY SHADING HIGHLIGHTS OUR PROPOSED METHODS (IPGA, IPGA-R).

VLM model	MF-it		MF-ii		CoA		IPGA		IPGA-R	
	ASR \uparrow	CleanACC \uparrow	ASR \uparrow	CleanACC \uparrow	ASR \uparrow	CleanACC \uparrow	ASR \uparrow	CleanACC \uparrow	ASR \uparrow	CleanACC \uparrow
BLIP2	0.7023	0.7033	0.6404	0.7249	0.8163	0.6094	0.8300	0.8056	0.8329	0.8516
InstructBLIP	0.5944	0.8028	0.5765	0.7737	0.7681	0.7014	0.8319	0.8047	0.8582	0.8601
MiniGPT-4	0.5897	0.7033	0.5737	0.6620	0.6455	0.6588	0.6657	0.7080	0.6685	0.7418
LLaVA	0.4704	0.7465	0.4610	0.7099	0.6122	0.6460	0.6629	0.7474	0.6545	0.7671
LLaVA-NeXT	0.4019	0.7840	0.3934	0.8066	0.5155	0.7399	0.5390	0.8225	0.5239	0.8344

Target: The crate to the right of the apples is made of metal.
 Target question (Q1): What type of material is the crate to the right of the apples made of?
 Unrelated question (Q2): Do you see ripe apples in this image?



(Clean) Q1: The crate to the right of the apples is made of wood.
 (Clean) Q2: Yes, I see ripe apples in this image.
 (Adv.) Q1: The crate to the right of the apples is made of **metal**.
 (Adv.) Q2: Yes, I see ripe apples in this image.

(a) MiniGPT-4

Target: The color of this car is red.
 Target question (Q1): What is the color of this car?
 Unrelated question (Q2): Do you see any small birds or dogs?



(Clean) Q1: The color of the car in the image is black.
 (Clean) Q2: No, the image features a large bird, specifically a crane, standing next to a car.
 (Adv.) Q1: The color of the car in the image is **red**.
 (Adv.) Q2: No, the image features a large bird, specifically a tall ostrich, standing next to a car.

(b) LLaVA

Target: The shoe is black.
 Target question (Q1): Is the shoe black or blue?
 Unrelated question (Q2): What is the mountain covered in?



(Clean) Q1: The shoe in the image is blue.
 (Clean) Q2: The mountain in the image is covered with snow.
 (Adv.) Q1: The shoe in the image appears to be **black**.
 (Adv.) Q2: The mountain in the image appears to be covered with snow.

(c) LLaVA-NeXT

Fig. 4. Visualization of the attack results of our IPGA-R on various open-source VLMs. We show the adversarial target text, target question, and unrelated question above the image, and display the visual question-answering results of the original image and adversarial example below the image. The fine-grained attack successfully transfers to models without a Q-Former module, such as LLaVA and LLaVA-NeXT, producing the target answer for the targeted question while preserving correct answers for unrelated questions, demonstrating strong transferability across different VLM architectures.

8/255, the resulting adversarial images remain visually imperceptible. The visualizations illustrate that our method achieves strong attack effectiveness and exhibits transferability across VLMs with different architectures.

Quantitative results of fine-grained attack performance.

In Table II, we evaluate the effectiveness of our proposed IPGA and IPGA-R in generating black-box adversarial images against VLMs for the fine-grained visual question-answering task. Unlike global targeted attacks that disrupt the entire image content, fine-grained attacks manipulate answers to specific questions while preserving unrelated information, requiring a more precise understanding of the image. Such attacks have practical implications. For instance, in autonomous driving, an attacker may alter the interpretation of a specific road sign or pedestrian without affecting other objects. Similarly, in VLM-powered robotics, an attack could target a specific object while leaving the rest of the scene unchanged to enhance stealthiness. We use the balanced validation set of GQA [18]. For each image, we select one question as the targeted VQA prompt and generate a false answer using GPT-4o as the adversarial target. To assess whether the attack preserves unrelated content, we pair each targeted question with an irrelevant clean question from GQA and use its original answer for evaluation. This setup allows us to analyze the granularity of the targeted attack and evaluate if adversarial modifications

disrupt unrelated content. We report the Attack Success Rate (ASR) for the targeted question and Accuracy (CleanACC) for the clean question, following the official evaluation protocol. The results show that our IPGA consistently achieves higher ASR and CleanACC across all VLMs compared to baseline methods, demonstrating its effectiveness in fine-grained targeted attacks and its ability to preserve unrelated content by leveraging the Q-Former’s fine-grained feature extraction for precise adversarial perturbations. Furthermore, IPGA-R achieves the highest CleanACC across all VLMs, providing additional improvement in preserving unrelated content over IPGA.

Qualitative results of fine-grained attack performance.

Figure 4 illustrates the effectiveness of our proposed IPGA-R in performing targeted fine-grained attacks while preserving unrelated content on open-source VLMs, including MiniGPT-4, LLaVA, and LLaVA-NeXT, which represent different architectures. Notably, the fine-grained attack also transfers successfully to models without a Q-Former module, such as LLaVA and LLaVA-NeXT, producing the target answer for the targeted question while preserving the correct answer for unrelated questions, demonstrating strong transferability across different VLM architectures.

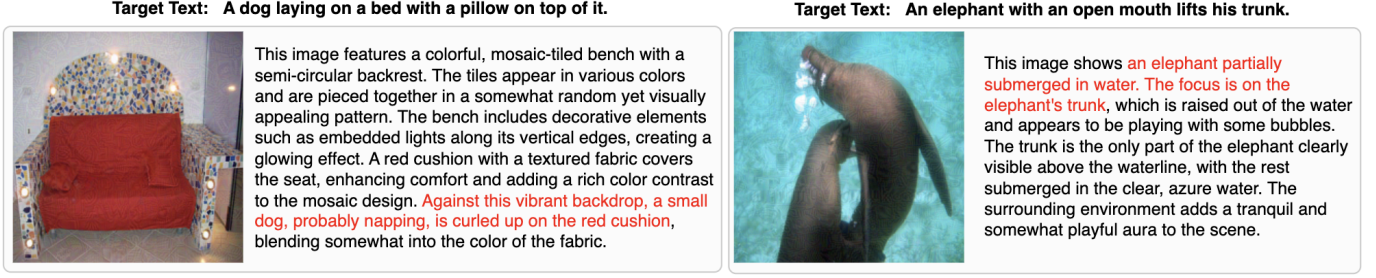


Fig. 5. Example responses from GPT-4o to global targeted attacks generated by our IPGA.

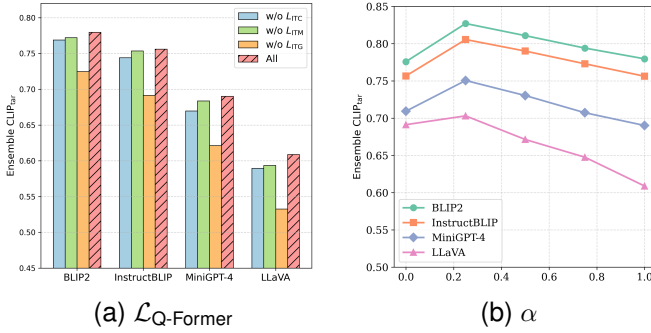


Fig. 6. The left figure displays the attacking ability of each loss component in $L_{Q-Former}$. The right figure displays the attacking ability of the proposed IPGA with different α .

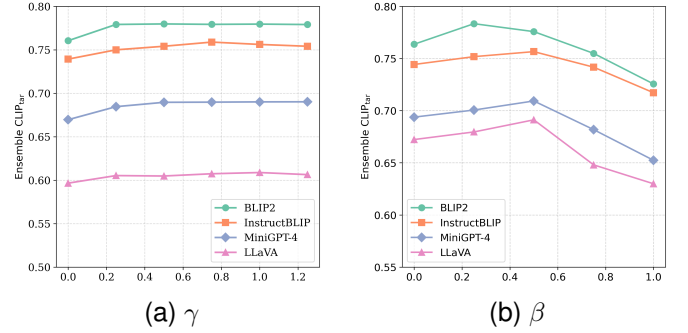


Fig. 7. The left figure displays the attacking ability of the proposed IPGA with different γ . The right figure displays the attacking ability of the proposed IPGA with different β .

C. More Analysis

Quantitative attack results on commercial VLMs. We evaluated fine-grained attack performance on 100 images from the GQA dataset. Table III reports the ratio of successfully attacked questions (ASR) and correctly answered unrelated clean questions (CleanACC) for Google Gemini and OpenAI GPT. IPGA achieves the highest ASR across all models, IPGA with Residual Query Alignment (IPGA-R) achieves the highest CleanACC while maintaining attack success that still surpasses the baseline methods. These results indicate that RQA module effectively balances attack strength and content preservation.

Qualitative attack results on commercial VLMs. To further illustrate the effectiveness of the proposed IPGA, Figure 5 presents qualitative results of adversarial images generated by our method. The images are evaluated using GPT-4o with the prompt ‘‘What is the content of the image?’’. Model responses highlighted in red correspond to the target content, clearly demonstrating the global attack impact of IPGA on commercial VLMs.

D. Ablation Study

Influence of loss components in $L_{Q-Former}$. We analyze the contribution of different loss components in $L_{Q-Former}$ by conducting experiments with $L_{Q-Former}$ alone on BLIP-2, InstructBLIP, MiniGPT-4, and LLaVA. The results of global attacks on the image captioning task are presented in Figure 6a. The findings show that all loss components contribute to the overall attack effectiveness, with the image-grounded text generation loss \mathcal{L}_{ITG} exerting the greatest influence.

TABLE III
QUANTITATIVE PERFORMANCE COMPARISON ON COMMERCIAL VLMs.
THE BOLD NUMBERS INDICATE THE BEST RESULTS, WHILE THE GRAY SHADING INDICATES OUR PROPOSED METHOD.

	OpenAI GPT		Google Gemini	
	ASR \uparrow	CleanACC \uparrow	ASR \uparrow	CleanACC \uparrow
MF-it	15%	90%	8%	89%
MF-ii	14%	87%	7%	91%
CoA	18%	86%	8%	85%
IPGA	24%	87%	15%	91%
IPGA-R	22%	92%	12%	96%

Influence of clean text deviation weights γ and β . To evaluate the influence of clean text deviation, Figure 7a presents the effect of varying γ in $L_{Q-Former}$ across the values $\{0, 0.25, 0.5, 0.75, 1, 1.25\}$. We observe that the CLIP score is lowest when $\gamma = 0$, while it generally reaches its maximum at $\gamma = 1$. This indicates that incorporating the original text deviation in $L_{Q-Former}$ enhances the effectiveness of targeted adversarial attacks. Figure 7b illustrates the influence of β in $L_{Encoder}$ (0, 0.25, 0.5, 0.75, 1), with $\beta = 0.5$ generally yielding the best performance.

Influence of the balance hyperparameter α . Figure 6b examines the impact of α , which controls the balance between $L_{Q-Former}$ and $L_{Encoder}$ in global attack using image captioning task. We evaluate $\alpha \in \{0, 0.25, 0.5, 0.75, 1\}$ and observe that the CLIP score peaks at $\alpha = 0.25$, indicating that both encoder loss and Q-Former loss play crucial roles in attack success for global attack.

VI. CONCLUSION

In this paper, we propose the Intermediate Projector Guided Attack (IPGA), a novel framework for targeted adversarial attacks on VLMs. By leveraging the intermediate pretraining stage of the Q-Former projector, which transforms global image embeddings into fine-grained visual features via cross-attention, IPGA achieves enhanced attack performance and transferability across VLMs with diverse architectures, and enables more precise and disentangled adversarial perturbation compared to conventional encoder-level attacks. To further enhance the preservation of unrelated image content, we introduce the Residual Query Alignment (RQA) module, which constrains residual query tokens to remain close to their clean counterparts, thereby enabling more precise adversarial manipulations. We evaluate IPGA on global targeted attacks using ImageNet-1K with MS-COCO captions and on fine-grained attacks using the visual question-answering task on GQA. Our results show that IPGA consistently outperforms existing targeted attack methods across both scenarios. Incorporating RQA (IPGA-R) further improves the preservation of unrelated content, yielding more controlled and realistic adversarial manipulations. Furthermore, our attack demonstrates successful transfer to commercial models, including Google Gemini and OpenAI GPT, highlighting its practical impact and revealing critical vulnerabilities in VLMs.

REFERENCES

- [1] J. Li, D. Li, S. Savarese, and S. Hoi, “Blip-2: Bootstrapping language-image pre-training with frozen image encoders and large language models,” in *International conference on machine learning*. PMLR, 2023, pp. 19 730–19 742.
- [2] H. Liu, C. Li, Q. Wu, and Y. J. Lee, “Visual instruction tuning,” *Advances in neural information processing systems*, vol. 36, 2024.
- [3] H. Lu, W. Liu, B. Zhang, B. Wang, K. Dong, B. Liu, J. Sun, T. Ren, Z. Li, H. Yang *et al.*, “Deepseek-vl: towards real-world vision-language understanding,” *arXiv preprint arXiv:2403.05525*, 2024.
- [4] D. Driess, F. Xia, M. S. Sajjadi, C. Lynch, A. Chowdhery, B. Ichter, A. Wahid, J. Tompson, Q. Vuong, T. Yu *et al.*, “Palm-e: An embodied multimodal language model,” *arXiv preprint arXiv:2303.03378*, 2023.
- [5] H. Wang, K. Dong, Z. Zhu, H. Qin, A. Liu, X. Fang, J. Wang, and X. Liu, “Transferable multimodal attack on vision-language pre-training models,” in *2024 IEEE Symposium on Security and Privacy (SP)*. IEEE Computer Society, 2024, pp. 102–102.
- [6] X. Cui, A. Aparcedo, Y. K. Jang, and S.-N. Lim, “On the robustness of large multimodal models against image adversarial attacks,” in *Proceedings of the IEEE/CVF Conference on Computer Vision and Pattern Recognition*, 2024, pp. 24 625–24 634.
- [7] C. H. Wu, R. Shah, J. Y. Koh, R. Salakhutdinov, D. Fried, and A. Raghunathan, “Dissecting adversarial robustness of multimodal lm agents,” *arXiv preprint arXiv:2406.12814*, 2024.
- [8] Y. Zhao, T. Pang, C. Du, X. Yang, C. Li, N.-M. M. Cheung, and M. Lin, “On evaluating adversarial robustness of large vision-language models,” *Advances in Neural Information Processing Systems*, vol. 36, 2024.
- [9] Q. Guo, S. Pang, X. Jia, Y. Liu, and Q. Guo, “Efficient generation of targeted and transferable adversarial examples for vision-language models via diffusion models,” *IEEE Transactions on Information Forensics and Security*, 2024.
- [10] P. Xie, Y. Bie, J. Mao, Y. Song, Y. Wang, H. Chen, and K. Chen, “Chain of attack: On the robustness of vision-language models against transfer-based adversarial attacks,” *arXiv preprint arXiv:2411.15720*, 2024.
- [11] A. Radford, J. W. Kim, C. Hallacy, A. Ramesh, G. Goh, S. Agarwal, G. Sastry, A. Askell, P. Mishkin, J. Clark *et al.*, “Learning transferable visual models from natural language supervision,” in *International conference on machine learning*. PmLR, 2021, pp. 8748–8763.
- [12] J. Zheng, C. Lin, J. Sun, Z. Zhao, Q. Li, and C. Shen, “Physical 3d adversarial attacks against monocular depth estimation in autonomous driving,” in *Proceedings of the IEEE/CVF Conference on Computer Vision and Pattern Recognition*, 2024, pp. 24 452–24 461.
- [13] W. Dai, J. Li, D. Li, A. Tiong, J. Zhao, W. Wang, B. Li, P. Fung, and S. Hoi, “InstructBLIP: Towards general-purpose vision-language models with instruction tuning,” in *Thirty-seventh Conference on Neural Information Processing Systems*, 2023. [Online]. Available: <https://openreview.net/forum?id=vvoWPYqZJA>
- [14] D. Zhu, J. Chen, X. Shen, X. Li, and M. Elhoseiny, “Minigt-4: Enhancing vision-language understanding with advanced large language models,” *arXiv preprint arXiv:2304.10592*, 2023.
- [15] Z. Qi, Y. Fang, Z. Sun, X. Wu, T. Wu, J. Wang, D. Lin, and H. Zhao, “Gpt4point: A unified framework for point-language understanding and generation,” in *Proceedings of the IEEE/CVF Conference on Computer Vision and Pattern Recognition*, 2024, pp. 26 417–26 427.
- [16] J. Deng, W. Dong, R. Socher, L.-J. Li, K. Li, and L. Fei-Fei, “Imagenet: A large-scale hierarchical image database,” in *2009 IEEE conference on computer vision and pattern recognition*. Ieee, 2009, pp. 248–255.
- [17] T.-Y. Lin, M. Maire, S. Belongie, J. Hays, P. Perona, D. Ramanan, P. Dollár, and C. L. Zitnick, “Microsoft coco: Common objects in context,” in *Computer vision—ECCV 2014: 13th European conference, zurich, Switzerland, September 6-12, 2014, proceedings, part v 13*. Springer, 2014, pp. 740–755.
- [18] D. A. Hudson and C. D. Manning, “Gqa: A new dataset for real-world visual reasoning and compositional question answering,” in *Proceedings of the IEEE/CVF conference on computer vision and pattern recognition*, 2019, pp. 6700–6709.
- [19] J. Achiam, S. Adler, S. Agarwal, L. Ahmad, I. Akkaya, F. L. Aleman, D. Almeida, J. Altschmidt, S. Altman, S. Anadkat *et al.*, “Gpt-4 technical report,” *arXiv preprint arXiv:2303.08774*, 2023.
- [20] R. Ramos, B. Martins, D. Elliott, and Y. Kementchedjhi, “Smallcap: lightweight image captioning prompted with retrieval augmentation,” in *Proceedings of the IEEE/CVF Conference on Computer Vision and Pattern Recognition*, 2023, pp. 2840–2849.
- [21] W. Wang, Q. Lv, W. Yu, W. Hong, J. Qi, Y. Wang, J. Ji, Z. Yang, L. Zhao, S. XiXuan *et al.*, “Cogvlm: Visual expert for pretrained language models,” *Advances in Neural Information Processing Systems*, vol. 37, pp. 121 475–121 499, 2024.
- [22] L. Liu, D. Yang, S. Zhong, K. S. S. Tholeti, L. Ding, Y. Zhang, and L. Gilpin, “Right this way: Can vlms guide us to see more to answer questions?” *Advances in Neural Information Processing Systems*, vol. 37, pp. 132 946–132 976, 2024.
- [23] Q. Sun, Y. Fang, L. Wu, X. Wang, and Y. Cao, “Eva-clip: Improved training techniques for clip at scale,” *arXiv preprint arXiv:2303.15389*, 2023.
- [24] P. Wang, S. Bai, S. Tan, S. Wang, Z. Fan, J. Bai, K. Chen, X. Liu, J. Wang, W. Ge *et al.*, “Qwen2-vl: Enhancing vision-language model’s perception of the world at any resolution,” *arXiv preprint arXiv:2409.12191*, 2024.
- [25] H. Liu, C. Li, Y. Li, B. Li, Y. Zhang, S. Shen, and Y. J. Lee, “Llava-next: Improved reasoning, ocr, and world knowledge,” January 2024. [Online]. Available: <https://llava-vl.github.io/blog/2024-01-30-llava-next/>
- [26] S. Han, C. Lin, C. Shen, Q. Wang, and X. Guan, “Interpreting adversarial examples in deep learning: A review,” *ACM Computing Surveys*, vol. 55, no. 14s, pp. 1–38, 2023.
- [27] A. Madry, A. Makelov, L. Schmidt, D. Tsipras, and A. Vladu, “Towards deep learning models resistant to adversarial attacks,” *arXiv preprint arXiv:1706.06083*, 2017.
- [28] K. Liang, X. Dai, Y. Li, D. Wang, and B. Xiao, “Improving transferable targeted attacks with feature tuning mixup,” in *Proceedings of the Computer Vision and Pattern Recognition Conference*, 2025, pp. 25 802–25 811.
- [29] M. Shen, C. Li, Q. Li, H. Lu, L. Zhu, and K. Xu, “Transferability of white-box perturbations: query-efficient adversarial attacks against commercial dnn services,” in *33rd USENIX Security Symposium (USENIX Security 24)*. USENIX Association, 2024, pp. 2991–3008.
- [30] J. Zhang, Q. Yi, and J. Sang, “Towards adversarial attack on vision-language pre-training models,” in *Proceedings of the 30th ACM International Conference on Multimedia*, 2022, pp. 5005–5013.
- [31] D. Lu, Z. Wang, T. Wang, W. Guan, H. Gao, and F. Zheng, “Set-level guidance attack: Boosting adversarial transferability of vision-language pre-training models,” in *Proceedings of the IEEE/CVF International Conference on Computer Vision*, 2023, pp. 102–111.
- [32] J. Zhang, J. Ye, X. Ma, Y. Li, Y. Yang, J. Sang, and D.-Y. Yeung, “Anyattack: Towards large-scale self-supervised generation of targeted adversarial examples for vision-language models,” *arXiv preprint arXiv:2410.05346*, 2024.
- [33] J. Lin, C. Song, K. He, L. Wang, and J. E. Hopcroft, “Nesterov accelerated gradient and scale invariance for adversarial attacks,” in *International Conference on Learning Representations*.